This is the Pre-Published Version.

Z. Nan, A.A. Khan, X. Zhang, L. Jiang, X. Huang, A. Usmani (2023) *Fire Spread and Burning Dynamics of Non-uniform Wood Cribs for Evolved Design Fire Scenarios*, **Fire Safety Journal**, 140, 103840. https://doi.org/10.1016/j.firesaf.2023.103840

Fire Spread and Burning Dynamics of Non-uniform Wood Crib for Evolved Design Fire Scenarios

Zhuojun Nan[1], Aatif Ali Khan[1,2], Xiaoning Zhang[1], Liming Jiang[1,*], Xinyan Huang[1,*], Asif Usmani[1]

[1]*Research Centre for Fire Safety Engineering, Department of Building Environment and Energy Engineering, The Hong Kong Polytechnic University, Hong Kong, China*

[2]*Department of Civil and Natural Resources Engineering, University of Canterbury, New Zealand*

** Corresponding to liming.jiang@polyu.edu.hk; xy.huang@polyu.edu.hk*

Abstract:

The 'travelling fire' models have been used to describe the localised and travelling burning of uniform fuel bed in large open-plan building space. However, fuel is typically distributed non-uniformly in the built environment, leading to complex fire spread behaviours. This paper investigates the effect of non-uniform fuel load distribution on fire development in a sufficiently-ventilated space. A series of fire tests up to 3.5 MW with different wood crib layouts are categorised into two types, i.e., non-uniform and continuous, and non-uniform and discontinuous. The leading and trailing edges of the flame, height of flame, and fire spread rates are estimated using visual evidence. The non-uniform fuel load distribution fundamentally changes the spreading behaviour of fire. On a continuous wood crib, the fire spread rate and fire size are generally proportional to the fuel load density when the arrangement of the wood crib is similar. However, when wood cribs are discontinuous, the fire dynamics depend more on the localised burning size and gaps between fuels. Furthermore, very distinct fire behaviours were observed for fuel loads with different porosity. This work reveals the possible under-estimation of fire hazards of assuming evenly distributed fuel load and suggests considering design fire scenarios of non-uniform fuel load distribution in the performance-based fire safety design.

Keyword: *Flame spread; Fuel load distribution; Large-scale fire; Performance-based design.*

1. Introduction

The 'travelling' nature of fire within the large open-plan space poses severe challenges to the fire safety of modern constructions. The concept of 'travelling fire' was proposed to characterise fires that may burn locally and spread within the large compartments since global flashover does not always occur. When being heated by a 'travelling fire', it raised concerns on the local heating and cooling, which may induce localised failure of key structural components such as connection failures potentially leading to structural collapses as found from the WTC fire [1].

Since 1990s, over thirty large-scale compartment fire experiments of the open-plan type have been conducted to investigate the fire dynamics and thermal impact, which were thereafter found of non-homogenous temperature distribution differing from the conventional small compartment fires [2,3]. In recent years, various full-scale large compartment fire tests have been conducted with particular interest on travelling behaviours, including Veselí Travelling Fire Test (2011) [4], Edinburgh Tall Building Fire Tests (2013) [5], Malveira Fire Test (2014) [6], Guttasjön Fire Test (2018) [7], Large-scale experiments x-ONE (2017) [8] and x-TWO (2019) [9], etc. Most of the existing large-scale travelling fire tests adopted a uniform fuel load distribution to simplify the fire tests aiming for explicit travelling behaviour [10,11]. The main parameters of the fuel beds in these fire experiments are summarized in Table 1. As shown in Table 1, different fire modes were perseverated in the existing fire experiments, e.g., travelling fire, growing fire, zonal intense burning (i.e., rapid spread of fire in a part of large open-plan compartment), and fire decay. The fire behaviour shown in the existing full-scale fire tests is characterized by analysing the test data and observation [12,13]. Furthermore, a quantitative index of fire mode can be derived from the measurement of travelling velocity and the ratio of the velocity of the flame leading edge to that of the trailing edge [6]. For example, the fire behaviours observed in the x-ONE and x-TWO fire tests (2017, 2019). Both tests were performed in a compartment of a size of 35.5 m (L)×10.8 m (W)×3.19 m (H) with uniformly distributed wood cribs. The fuel load densities (fuel load per unit area on floor) of x-ONE is 370 MJ/m^2 [8], while in x-TWO the values are 355 MJ/m^2 for Part 1 and 249 MJ/m^2 for Part 2 [9]. These tests demonstrated the effect of the fuel load density on the spread rate of fire on uniform wood crib beds. The x-ONE test of higher fuel load density produced a faster fire spread, and the fire lasted around 25 min. In the x_ONE, the fire spread with gradually accelerating, as a growing fire leading to zonal intense burning after 10 mins [8]. There was an increase in fire size from approximately 4 MW at the beginning to around 70 MW at the peak [8]. Whereas the x-TWO Part 2 test of a lower fuel load density lasted longer for around 180 min with an average spread rate of 0.22 m/min. The time-variant total release rate could be calculated based on the heat release rate (HRR) per unit length and the experimental observation of the location of the leading and trailing edges [8].

To characterise the fire spread modes in the large compartment, from the Malveira Fire Test results Hidalgo et al. [6] proposed a methodology based on the velocity of flame leading edge (V_S) and the trailing edge(V_{BO}). It describes the various fire spread phenomenon according to ratio of these velocities, such as fully-developed fire ($V_S/V_{BO} \rightarrow \infty$), growing fire ($V_S/V_{BO} > 1$), and a 'travelling fire' ($V_S/V_{BO} \approx 1$). Gupta et al. [13,14] further assimilated large-scale compartment fire experiments and studied the role of ratio of the leading edge and trailing edge velocities, which offers a pathway for defining design fire scenarios in large open spaces representing more realistic dependencies of fire characteristics. In open-plan compartments, fire spread is controlled by the energy balance at the fuel surface. This energy balance consists of two components: the external heat fluxes that preheat the fuel correspond to slow accelerations; and the flame heat fluxes corresponding to sudden fire spread [14].

The travelling fire methodologies are evolving, which currently assume a constant fire spread rate of the localised burning for engineering use, which include the earliest Clifton's travelling fire model [15], Travelling Fires Methodology (TFM) [16] and an Extended Travelling Fire Methodology (ETFM) framework [17]. While the travelling fire models were proposed to represent potentially the worse scenarios comprising locally intense heating and subsequent cooling, it is of significant importance to consider the non-uniformity along the travelling trajectory. For instance, the travelling behaviour of time-variant fire spread rates and fire sizes using linearized models can be considered while maintaining the simplicity of engineering expression. The existing travelling fire model, which incorporates comprising constant fire size and travelling behaviour, is unsophisticated and may cause a substantial underestimation of the localised fire impact. The natural fire model comprises time-variant and travelling behaviour models and localised fire models of various modes has been proposed [12]. The fire scenarios of time-variant travelling can lead to locally higher temperatures of more than 200 ^{o}C in steel beams compared to the cases assuming constant travelling, which can potentially cause unexpected local failure of structural systems. In reality, the distribution of fuel load is usually non-uniform and discontinuous. A localised fire of a larger size and longer heating duration may occur when the fuel is more densely distributed locally but the fuel load density on floor remains the same. This may cause localised damage of structural components possibly leading to structural failure. In the future version of design fire models, the necessity of considering the non-uniformity for fuel distribution and travelling behaviour are recognized.

Several researchers have investigated the fire spread behaviours over discrete fuel arrays [5,18,19], including pool fires, wood cribs and furniture. For example, Kirby et al. [18] experimentally investigated the fire spread of discrete wood cribs in a compartment. Nine fire tests were carried out to investigate a variety of fire conditions, such as fire load and ventilation. The experimental data was then used to further develop parametric curves for safe realistic prediction. Besides, the first of the Dalmarnock Fire Tests was a full-scale fire experiment with realistic fuel distribution that successfully developed into an unrestrained

post-flashover fire [19]. The characterisation of the fire has also allowed for the subsequent analysis of structural behaviour with the fire development. In a real building fire, the worst scenario is associated with the failure of key structural components, which is more likely caused by local heating of high intensity and long duration fire, i.e., a larger fire size and a lower fire spread rate over the fuel bed. Hence, it is imperative to characterise fire spread on non-uniform fuel bed for worse design fire scenarios.

This study is carried out for the above purpose, experimentally investigating the fire spread over non-uniform fuel bed. Five full-scale wood-crib fire tests were conducted in a sufficiently-ventilated space with the representative fuel load setup, i.e., non-uniform and continuous, and non-uniform and discontinuous wood crib layouts. The tests feature the non-uniform fuel load distribution to investigate the fire spread and burning behaviours (i.e., the development of fire spread rate and fire size) and its impact on surroundings (i.e., temperature and heat flux).

2. Experimental setup

The experimental work is aimed at investigating and emphasising the importance of the fire spread on non-uniform fuel beds in a large open-plan space. The primary objectives of the tests are: (1) to study the effect of fuel distribution on a natural spreading fire, (2) to investigate the correlation of local fuel density with spread rate, (3) and to measure the fire impact. The five full-scale fire tests were carried out in the fire laboratory of Sichuan Fire Research Institute (Sichuan, China), which is a 140 m-long tunnel of 8 m-wide and 5 m-high. The selected test region nearby the south opening of the tunnel is 10 m-long, 8 m-wide and 4.5 m-high with the protected inner section, as shown in Fig. 4.

It was chosen to represent a ‘slice’ of a large open-plan office with sufficient ventilation. The aspect ratio of the selected test region is approx. 1.3 (estimated as 10 m over 8 m), which is within a reasonable range (i.e., 1.3 - 4.5 [11]) for fuel-controlled fire spread according to the existing large-scale open-plan compartment fire experiments. The average ambient temperature was 20 ^{o}C ± 1 ^{o}C inside the tunnel. The design of this test compartment (i.e., the region of the tunnel nearby the south opening) was similar to the test compartment of the BST/FRS 1993 Natural Fire Tests Series [18]. Here it is to observe the burning behaviour on wood crib when it is fuel-controlled, which has been found in the fire tests in large compartments exhibiting travelling fire behaviour [21]. The south opening and mechanical ventilation system (with a velocity of 2.5-3 m/s) were used to provide sufficient ventilation to efficiently ventilate smoke similar to the longitudinal ventilation in large and long open-plan space. In each test, the wood cribs were used as fuel beds and the typical formulation is shown in Figs. 1 and 2.

Table 1. Summary of fuel characteristics for the existing large-scale compartment fire experiments.

Experiment	Test	Compartment dimensions (m)	Fuel bed dimensions (m)	Fuel load density on floor (MJ/m^2)	Fuel load density on fuel bed (MJ/m^2) (means kg/m^2)	Stick thickness b (m)	Stick length l (m)	Number of sticks per layer n	Number of layers N	Stick spacing s (m)	Fire behaviour
Veselí Travelling Fire Test	Test1	13.4×10.4×4.0	8×3	173.5	1007.5 (57.5)	0.05	1	7	6	0.05	Growing → Zonal intense burning → Fire decay
Edinburgh Tall Building Fire Tests	Test1-2	17.8×4.9×2.0	16×3	480	872.2 (52.0)	0.05	1	10	4	0.05	Growing → Zonal intense burning
Malveira Fire Test	-	21×4.7×2.85	16.8×2.4	420	1028.1 (57.2)	0.05	1.2	10	3.5	0.05/0.15	Travelling → Growing → Zonal intense burning
Guttasjön Fire Test	-	18×6×3	15.2×2.5	310	881.1 (44.4)	0.045	1	10	4	-	Travelling
Large-scale experiments	x-ONE	35.5×10.8×3.19	29×6	370	815.3 (42.7)	0.03	1	4	11.5	-	Growing → Zonal intense burning
	x-TWO 1			355	782.2 (41.4)	0.03	1	4	11.5	-	Travelling → Growing → Zonal intense burning → Fire decay
	x-TWO 2			249	548.7 (30.7)	0.03	1	4	8.5	-	Travelling → Zonal intense burning → Fire decay

Table 2. The large-scale calorimeter benchmark experiments [20] of 'spruce' wood cribs with different sizes in SCFRI.

Test No.	Wood Crib L×W×H (m)	Stick thickness b (m)	Stick length l_i (m)	Stick length l_j (m)	Number of sticks per layer, n_i	Number of sticks per layer, n_j	Number of layers, N	Weight of wood crib (kg)	Peak HRR (kW)	Time to reach peak HRR (s)
1	0.45×0.75×0.5	0.05	0.75	0.45	5	8	10	48.1	333	1250
2	0.75×1.0×0.5	0.05	1	0.75	8	10	10	78.2	753	927
3	1.0×1.5×0.5	0.05	1.5	1	10	15	10	174	1551	1140

*i and j are used to refer to different directions.

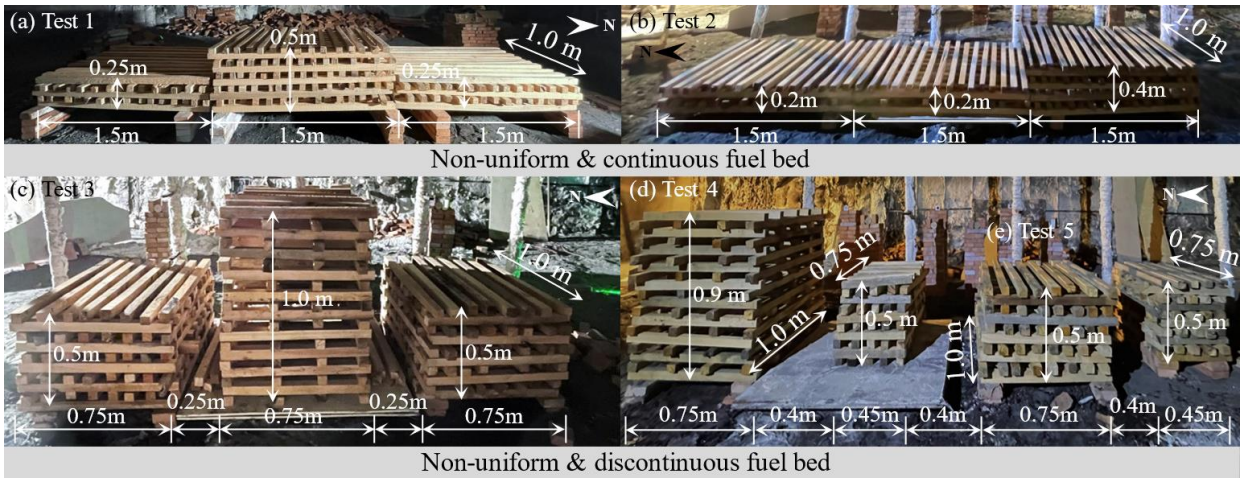

Fig. 1. Typical non-uniform wood-crib load setups.

Wood cribs were commonly adopted as fuel load in the past full-scale large compartment fire tests to investigate the travelling behaviours [4–9,22–24]. However, the fire laboratory of SCFRI limited the fire size (i.e., it cannot be larger than 10 MW). Therefore, the fuel beds in this experiment were not covering the floor which like the existing large-scale compartment fire experiments to present the characteristic fire load densities. The objective of this experiment is to investigate the fire spreading and burning dynamics of the non-uniform wood cribs which reflects the uneven distribution of fire loads in real buildings (to represent the realistic condition in buildings, where fuel load is unevenly distributed). In order of observation on site and control of variables, the total wood cribs across the floor have been reduced. The wood cribs were distributed at the centre of the well-protected test region nearby the south opening of the tunnel. Each fuel bed comprised multiple stacks of wood cribs. The main parameters of the fuel beds in this experiment are fuel load density per unit area of the wood cribs (MJ/m^2, equivalent to kg/m^2) and the porosity (which relevant to stick spacing (m)). The design of the wood cribs referred to the existing large-scale compartment fire experiments as aforementioned (see Table 1). In our research, the wood cribs of 'spruce' were used as the fuel source. The average density of the wood was 430 kg/m^3 with a moisture content of 14 ± 2%. The moisture meter (GM610) was used to measure the wet moisture content of wood sticks. Prior to each test, a sample of 20 wood sticks which were collected on the day was weighed and measured to obtain representative average wood density and moisture. The heat release rate of 'spruce' wood cribs with different sizes measured in SCFRI by conducting large-scale calorimeter benchmark experiments [20], as shown in Table 2.

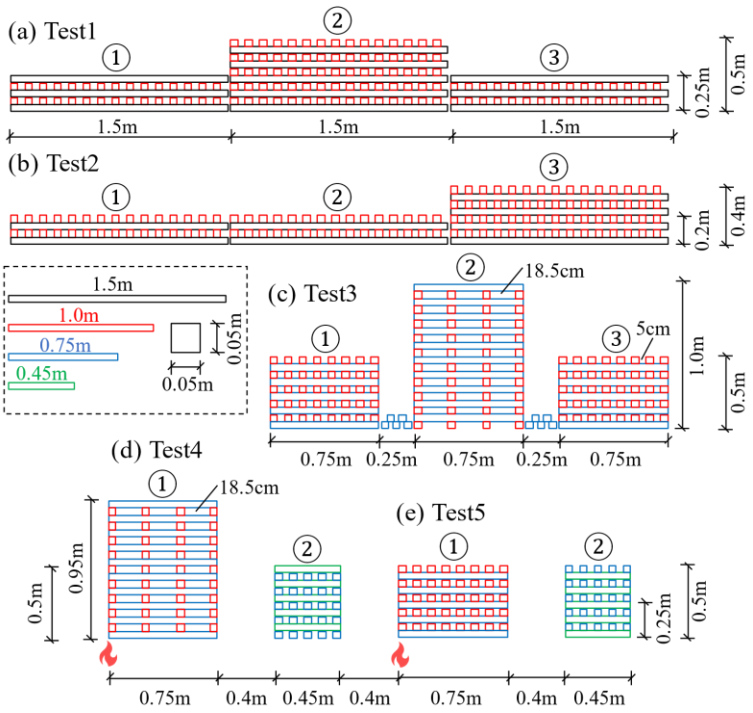

Fig. 2. Schematic of fuel load set up for each test.

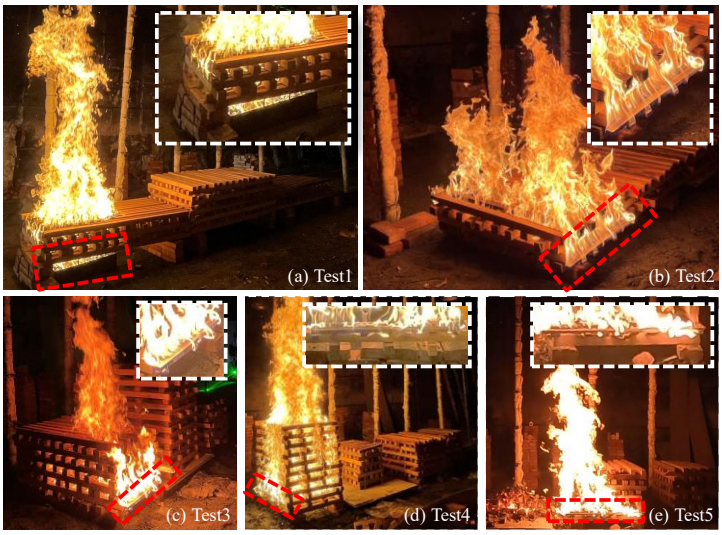

Fig. 3. The set-up of ignitor for each test.

To ignite the wood crib blocks, a pool (60×60 cm^2) with 7 kg ethanol was placed as an ignitor in Test 1, whereas wood sticks soaked with heptane were used as the ignitor for the rest of the tests. The locations of wood stick ignitors are shown in Fig. 3 using red dashed boxes, which comprised 1 stick along the longitudinal direction and 4 sticks perpendicular to it placed at the bottom of the wood crib and each stick is 0.5 m long and of a cross-section area around 9 cm^2. The wood stick ignitors have different impact on the burning behaviour compared to the pool fire, e.g., acceleration of burning rate and fire spread rate, and

increase of local fire size. The observed durations of ignitors of each test have been marked in Fig. 9 and Fig. 10, which has limited effect on the fire travelling behaviour to adjacent wood brick. Due to sufficient ventilation along the longitudinal direction of the testing space, no significant smoke accumulation occurred, which corresponds to the premise of large compartment fires featuring fuel-controlled fire development. Based on the layout of wood cribs, the fire tests can be categorised into two basic types, i.e., non-uniform and continuous (Tests 1 and 2) and non-uniform and discontinuous (Tests 3, 4, and 5), as shown in Figs. 1 and 2. Table 3 shows the configurations of all tests.

The key design factors included fuel load density and layout of wood cribs (e.g., the height of wood cribs, the gap between wood cribs, the exposed surface area of the single wood crib and the porosity of wood cribs). For the layout of wood cribs, the exposed surface area of the single wood crib (A_s), the area of vertical shafts (A_v) and the porosity (Φ) [25–27] were calculated according to Eqs. (1) to (3), respectively.

$$A_s = n_i N_i (2b^2 + 4bl_i) + n_j N_j (2b^2 + 4bl_j) - (N - 1) n_i n_j b^2 \tag{1}$$

$$A_v = (l_i - bn_j)(l_i - bn_j) \tag{2}$$

$$\Phi = N^{0.5} b^{1.1} (A_v / A_s) \tag{3}$$

where b is the width of the square cross section of wood stick, N is the number of total layers (i.e., $N = N_i + N_j$), N_i and N_j are the number of layers, l_i and l_j are the length of wood sticks, n_i and n_j are the number of wood sticks in each layer with i and j for different directions.

The fuel load per unit area on single wood crib ($q_{w,k}$) was calculated according to Eqs. (4) and (5).

$$m = \rho V \tag{4}$$

$$q_{w,k} = \eta \Delta H_c m \tag{5}$$

where $\eta \approx 0.8$ is the combustion efficiency following EN 1991-1-2 [28], and $\Delta H_c = 18$ MJ/kg is estimated as the heat of combustion of wood [29], ρ is the density of the wood (averaged on 430 kg/m^3 in this experiment), V is the volume of wood in the single crib and m is the weight of the single crib.

The cross-section of all wood sticks was 5 cm × 5 cm but of different lengths 0.45 m, 0.75 m, 1.0 m and 1.5 m, for different wood crib blocks as shown in Fig. 2. For the tests with discontinuous fuel bed, the distances between wood crib blocks were prescribed as 0.25 m in Test 3, and 0.4m in Tests 4&5, as shown in Fig. 2.

In this experiment, the dimensions of the wood cribs were selected based on the SCFRI large-scale calorimeter benchmark experiments [20], e.g., 1.5×1.0×0.5 m^3, 0.75×1.0×0.5 m^3, and 0.45×0.75×0.5 m^3, as shown in Table 2. The total fuel load is limited to avoid a large fire which might cause permanent damage to the laboratory. Note that Test 2 is the control group for this experiment. In Test 1 and Test 2, the area of fuel bed is the same i.e., 3×1.5×1.0 m^2. However, the fuel load densities (either local fuel load density for

each wood crib or total volume of wood sticks, Test 1 is slightly higher than Test 2 due to technician's mistake) and the distribution of fuel loads (see Figs. 1 and 2) are different. Observing fire behaviour in Test 1 and Test 2, the effect of fuel load densities and fuel load distribution on the fire spread and burning dynamics of the continuous fuel bed can be found.

Aside from Test 1, the intended total volume of wood in the cribs for the rest of tests was the same, i.e., 0.6 m^3. Note that the gap between two wood crib blocks in Test 3 were to keep the total volume of wood identical to that of Test 2 (i.e., 0.6 m^3). When the fuel distribution is discontinuous with a gap between two wood crib blocks (i.e., 0.4 m), it was found that the fire size on crib 4-2 in Test 4 was too small (e.g., 0.7 MW of Crib 4-2 as shown in Fig. 11(a)) to ignite the adjacent wood crib. Then the third wood crib block was manually ignited, as shown in Figs. 2 and 3, which is then denoted as Tests 5. When the size of localised fire is large enough, the fire leaped from the ignited wood crib (i.e., Crib 4-1 and Crib 5-1) to the adjacent wood crib in Test 4 and Test 5, as shown in Figs. 7(b) and 7(c). Especially, wood cribs of geometry of 0.75×1.0×1.0 m^3 used in Test 3 (Crib 3-2) and Test 4 (Crib 4-1) adopted a larger spacing of 18.5 cm between the wood sticks, which is different from the spacing of 5 cm in other wood cribs. This is to investigate the effect of porosity while maintaining the same local fuel load density (i.e., $q_{w,k}$).

The details of fuel bed geometry with wood cribs are summarised in Table 3, where the size of each wood crib block, gaps between discontinued blocks, the volume of wood in the single crib (V), the fuel load density per unit area on single wood crib ($q_{w,k}$), the exposed surface of a single wood crib (A_s), the area of vertical shafts (A_v) and the porosity (Φ) are given. In each test, Crib 1 (corresponding to ① in Table 3) was ignited first, and then the fire spread to Crib 2 or Crib 3 (if existed) during the experiment. In the following discussion, Crib 1 of Test 2 may be denoted as Crib 2-1 for test comparison.

Table 3. Summary of fuel characteristics for each test.

Test No.	Wood Crib L×W×H (m)	Gap (m)	V (m^3)	$q_{w,k}$ (MJ/m^2) (means kg/m^2)	A_s (cm^2)	A_v (cm^2)	Φ
1	①1.5×1.0×0.25	NA	0.1875	774 (54)	138000	3750	0.3569
	②1.5×1.0×0.5	0	0.375	1548 (108)	272500	3750	0.2556
	③1.5×1.0×0.25	0	0.1875	774 (54)	138000	3750	0.3569
2	①1.5×1.0×0.2	NA	0.150	619 (43)	111250	3750	0.3959
	②1.5×1.0×0.2	0	0.150	619 (43)	111250	3750	0.3959
	③1.5×1.0×0.4	0	0.300	1238 (86)	218750	3750	0.2848
3	①0.75×1.0×0.5	NA	0.194	1600 (111)	141500	1750	0.2297
	②0.75×1.0×1.0	0.25	0.194	1600 (111)	150000	4125	0.7223
	③0.75×1.0×0.5	0.25	0.194	1600 (111)	141500	1750	0.2297
4	①0.75×1.0×0.95	NA	0.184	1517 (105)	142300	4125	0.7421
	②0.45×0.75×0.5	0.4	0.092	1686 (117)	67750	700	0.1919
5	①0.75×1.0×0.5	NA	0.194	1600 (111)	141500	1750	0.2297
	②0.45×0.75×0.5	0.4	0.092	1686 (117)	67750	700	0.1919

*NA - Not Applicable

The measuring instrumentation includes thermocouples, weighing scales, heat flux gauges and video cameras. Fig. 4 presents the experimental set-up of Test 2 as an example. The experimental set-up of Test1, Test3, Test 4 and Test 5 have been presented in the Appendix. 67 K-type thermocouples were installed to establish the spatial and temporal gas-phase temperature field. Heat flux gauges, including TS-34C (i.e., HF1 and HF3), HS-34CB (i.e., HF2) and thin skin calorimeters (TSC), were used to quantify the incident heat flux to solid surfaces, as shown in Fig. 4.

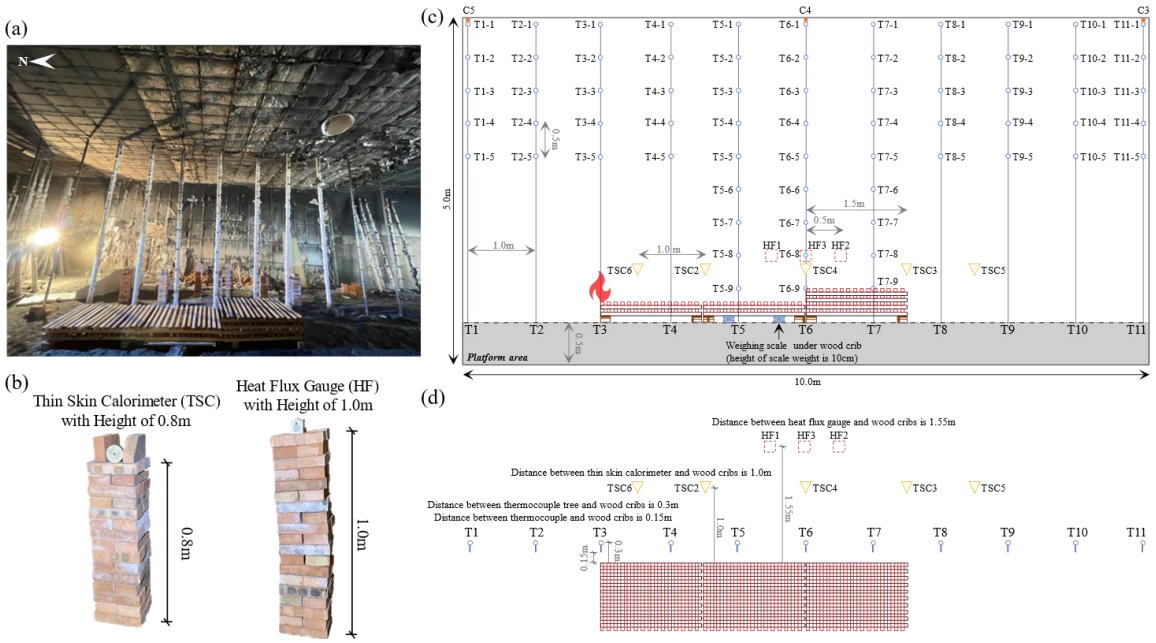

Fig. 4. The experimental set-up of Test 2. (a) Picture of Test 2. (b) Set-up of thin skin calorimeter (TSC) and heat flux gauge (HF). (c) Sketch with the location of sensors (elevation view). (d) Sketch with the location of sensors (plan view).

The mass loss of the wood cribs was monitored by the weighing scales (10 cm high) placed underneath the fuel bed, as shown in Fig. 5. The weighing scale with a maximum load capacity of 500 kg was calibrated on-site before the tests. In Tests 2-4, the mass of representative wood crib blocks was weighed, which includes Crib 2-2 (1.5×1.0×0.2 m^3) of 65.44 kg, Crib 3-2 (0.75×1.0×1.0 m^3) of 82.93 kg, Crib 4-2 (0.75×1.0×1.0 m^3) of 39.64 kg and Crib 5-1 (0.75×1.0×0.5 m^3) of 85.52 kg. As aforementioned the average density of the wood was 430 kg/m^3, and the measurement uncertainty of the weighing scale is ±2 kg. Except for the normal weighing function, the XK3190-AW1 also has a continuous weighing function which can record the mass every two seconds. Therefore, the XK3190-AW1 was set up in Test 2-4 to record the mass loss of the selected wood crib block for later heat release rate calculation. To determine and observe the development of fire flames over the wood crib bed (including the height and position of the plume as well as the locations of leading edge and trailing edge of burning region), the cameras at multiple locations were set up for recording. During each test, three cameras were deployed, comprising a Sony HD camcorder and

two GoPro cameras. The Sony HD camcorder was positioned on the northwest periphery of the selected test region, approximately 6.5 meters from the wood cribs. Utilising its zoom functionality, the camcorder monitored the progression of fire spread throughout each test. Concurrently, a GoPro camera was installed beside the western wall of the selected test region, positioned roughly 4 meters from the center of the wood cribs, with its lens facing them. This arrangement allowed for a more intimate and intuitive record of the fire spread process. To mitigate data loss due to potential camera shutdown from heat exposure during the experiment, the author manually holds an additional GoPro to continuously capture the proceedings. Prior to each experiment, camera parameters such as exposure and focal length were meticulously examined and adjusted as needed. Meanwhile, the experimental phenomenon was recorded manually at the test site. Ten thermocouple trees set near the fuel bed were also used as reference data for estimating the burning region and the flame height.

Fig. 5. The set-up of weighing scale (XK3190-AW1).

3. Results and discussion

3.1 The fire-spread behaviour

In each test, the fire behaviour over fuel bed has been recorded in videos and photos, which clearly exhibited a 'travelling' of localised burning. To calibrate and correct the camera for depth of field, thermocouple trees were used as a calibration target. The target was placed at the same distance and orientation as the test fuel bed, and images of the target were captured using multiple camera settings during the fire experiments. These images of the calibration target were then analysed to compute accurate information about the flame. In addition, observation data recorded by the experimenters on site was used for calibration. These steps helped to minimize measurement errors and enabled a more accurate analysis of fire behaviour.

The 'travelling' behaviour in the current experiments are unique, it is the first time non-uniform and discontinuous fuel load distribution is considered in tests. The images - captured during each test - have been provided as Figs. 6 and 7 for depicting the fire behaviour. Due to the limitation of pages, more images

of Test 1 and Test 2 have been presented in the Appendix (see Figs. A1 and A2). The videos of Test 2 and Test 3 as representative tests for each category have been provided as supplementary materials to the paper.

Fig. 6. Fire spread on continuous fuel bed (Tests 1&2).

For tests of continuous wood crib distribution, localised fires can be found on the crib blocks with the receding trailing edge of the burning region, as shown in Fig. 6(a) (Test 1) and Fig. 6(b) (Test 2). When the fire flames remained at the Crib 1-1 in Test 1 at 12 mins after the ignition, the flame height was approximately 1.3 m, while the burning length was around 1 m. When the fire on the Crib 1-2 was fully developed, a much higher fire plume was seen at 38 mins. Unlike Test 1, in Test 2, a slow and steady spread was observed (i.e., a 'travelling fire') from 20-85 mins. The burning length and flame height were also stable around 0.45 m and 0.6 m, respectively. After 85 mins, the fire intensity increased (re-growing) due to the flame approaching the Crib 2-3 of higher fuel density. The HRR increased, indicating that more fuel was available for combustion. Therefore, the observed increase in fire intensity was primarily due to the doubling of the fuel load in this area. The edge of the Crib 2-3 started the pyrolysis and got ignited. As the Cribs 2-2 and 2-3 joined the combustion, a peak fire length of 0.95 m was observed. Due to the higher fuel load density of Crib 3-2 (i.e., 1238 MJ/m^2 of Crib 2-3 which is doubled as Crib 2-2), a faster travelling fire appeared as the surface spread rate on the Crib 2-3 increased owing to the higher radiative heat from the larger localised fire.

For the category of discontinuous fuel distribution, Tests 3-5 (as shown in Fig. 7) investigated the effect of fuel layout (including the gaps between wood cribs and the porosity of the wood crib) on fire

spreading. As shown in Fig. 7, there is one noteworthy fact regarding the discontinuous fuel bed, which is that the ignition of the next wood crib always occurs at the top of the wood crib first. Hence, the observation of fire spread was based on the top of the wood crib. Test 3 demonstrated the possibly worse fire scenarios while the total fuel load is kept the same, i.e., the fire scenarios with locally higher fire impact could lead to structural failure. In Test 3 (Fig. 7(a)), the localised fire forming on the Crib 3-1 quickly ignited the Crib 3-2 (0.25 m gap) at 9.5 mins at the vertically exposed wood sticks (denoted as 'fire leaping'). The fire flames later formed a shape comprising two fire plumes interacting with each other (denoted as 'multi-centre fire'), and the flame height has exceeded 2.5 m (see Fig. 10a). At 25 mins, the fire size decreases following the decay at the Crib 3-1 and the Crib 3-3 was ignited but producing much smaller fire.

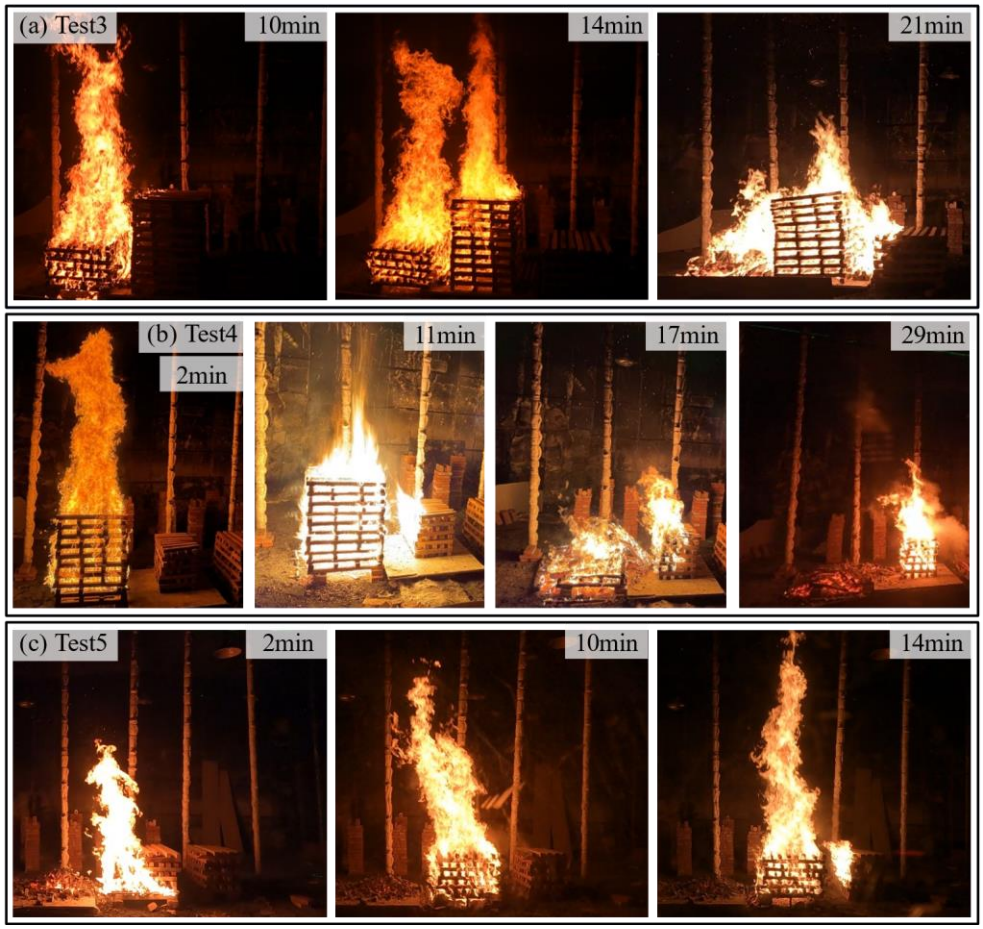

Fig. 7. Fire spread on discontinuous fuel bed (Tests 3-5).

A similar fire spread pattern was observed in Test 4 (Fig. 7(b)), which began with a large fire size on a heavier loaded wood crib similar to the Crib 3-2. The flame height nearly reached 3.0 m in 2 mins (see Fig. 7(b)), which is high enough to impinge the ceiling of typical buildings. The Crib 4-1 started to collapse at 12 mins and burnt out in around 18 mins. Since the Crib 4-2 was located with a 0.4 m distance between their facing edges, the ignition of the Crib 4-2 occurred at 10 mins. Unlike Test 4, Test 5 (Fig. 7(c)) adopted

wood crib blocks of the same height (0.5 m), whereas the gap remained the same (0.4 m). The fire development was limited on the Crib 5-1 until the Crib 5-2 was ignited 14 mins after the ignition.

3.2 Characteristics of fire spread

As mentioned in Section 3.1, the layout of fuel (including the continuity of fuel bed (continuous/discontinuous), the local fuel load density, the porosity of wood crib, the gap between wood cribs, etc.) fundamentally changed the fire-spread behaviour. Fig. 8 characterised the fire-spread behaviour with two typical formulations of fuel load distribution, i.e., non-uniform and continuous, and non-uniform and discontinuous. In general, when describing the travelling behaviour of fire in large compartments with uniform fuel load distribution, the locations of leading edge and trailing edge are characteristic variables, indicating the location of intense burning [2] (near field in travelling fire methodology) and the fire length. The velocity of the leading edge (V_S) and the trailing edge (V_{BO}) could be adopted to indicate the fire spread rate of 'travelling fire' with the continuous fuel load. Meanwhile, for non-uniform fuel load distribution, the fire impact of the burning region (e.g., fire size and burning duration) is also relevant to the local fuel load density and the HRR.

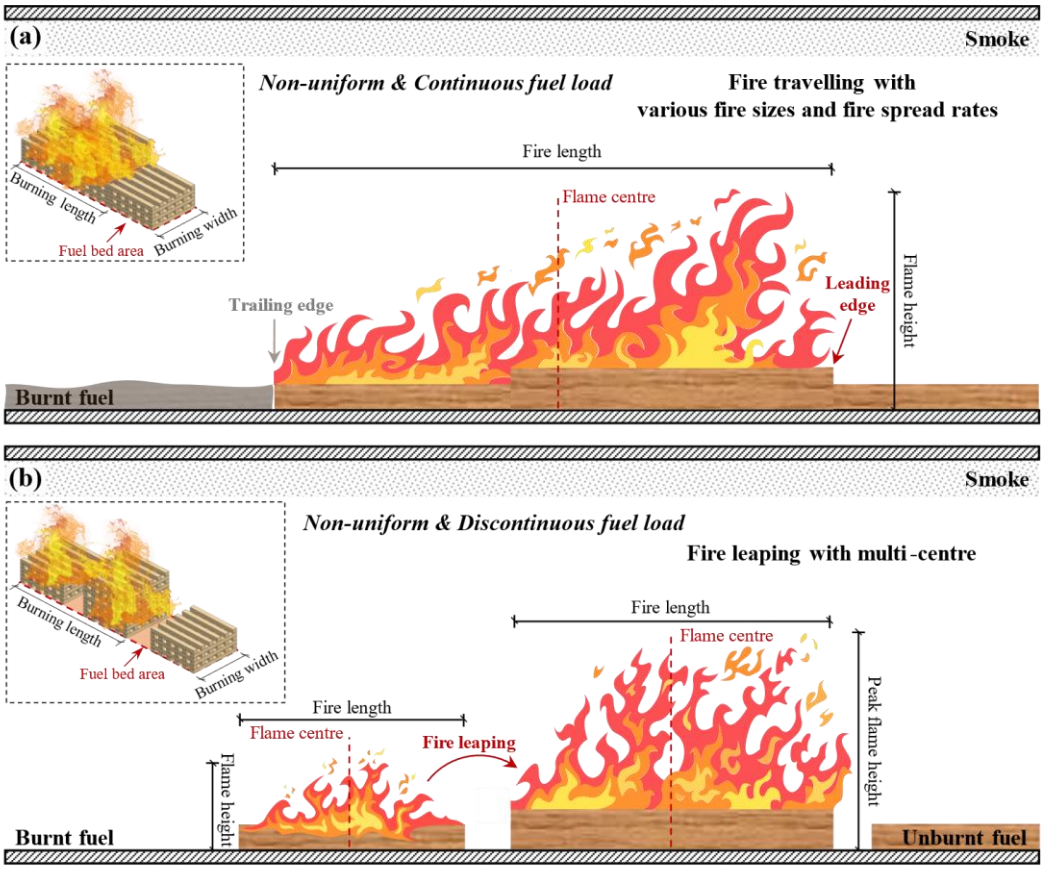

Fig. 8. Characterising of the fire-spread behaviour for two typical formulations of fuel load distribution. (a) Non-uniform and continuous. (b) Non-uniform and discontinuous.

Furthermore, considering the discontinuous fuel load distribution, 'multi-centre fire' occurred due to 'fire leaping' (i.e., the fire spread from the ignited wood crib to the surrounding wood cribs which created another fire plume and both wood cribs kept burning together). Hence, a constant fire spread rate did not appear on the discontinuous fuel bed. The leaping of the burning region along the discontinuous fuel load is also dependent on the local fuel load density and the porosity of wood cribs [2]. As shown in Fig. 8, the width of the fuel bed is defined as the width of the widest wood crib and the length of the burning region including the wood cribs and gaps. These fire spread behaviours observed during the tests are illustrated in Figs. 9 and 10.

As shown in Figs. 9 and 10, the travelling distance of fire is the relative distance between the ignition location and the leading edge/trailing edge [2]. The measurement of flame height is taken from the base of the wood crib to the top of the flame [30]. On the continuous but non-uniform wood crib bed (Tests 1&2), the travelling distance of the leading edge and the trailing edge are of similar incremental slopes, indicating the steady travelling fire. In Test 1 (Fig. 9(a)), the estimated fire spread rates represented by the velocity of leading edge and trailing edge are mostly below 2 mm/s. The similar values of V_S and V_{BO} suggest $V_S/V_{BO} \approx 1$, which is a quantitative criterion of travelling fire behaviour [6]. During the test, a plateau of flame height around 3.0 m occurred from 38 mins to 45 mins, when the fire plume was on the Crib 1-2. As shown in Fig. 9(a), when the fire spread from Crib 1-1 to Crib 1-2, the trailing edge just appeared. At this point, the largest burning length was observed as 1.5 m, which indicates that during the test the burning area was below 1.5 m^2 (with the burning width of 1.0 m). It might because that the powerful ignitor (i.e., the pool with ethanol) had an irresistible effect in Test 1.

In Test 2 (Fig. 9(b)), the 'travelling fire' mode is clearly shown when comparing the locations of leading edge and trailing edge of the localised burning. The spread rate of both edges are quite close, ranging from 0.5mm/s to 1.0 mm/s. This is due to the high heat losses of the test compartment, the pre-heating by the external heat flux ahead of the flame front is minimal [14]. The characteristic ratio V_S/V_{BO} is 0.5 to 2.0, roughly fulfilling the travelling fire criteria. When the fire plume reached the Crib 2-3 (after 90 mins since ignition), the largest value of the flame height and the fire length was observed (i.e., 2.0 m and 0.85 m, respectively, see Fig. 9(b)), as the Crib 2-3 had a higher $q_{w,k}$ = 1238 MJ/m^2 (see Table 3), which is twice of the fuel density of Cribs 2-1 and 2-2 in Test 2. Comparing with the values of Test 1 averaged at 0.8 mm/s, a lower fire spread rate averaged at 0.5 mm/s is found in Test 2 as shown in Fig. 9, and the fire spread rate is dependent on the fuel load density and the HRR but not in a linear relationship.

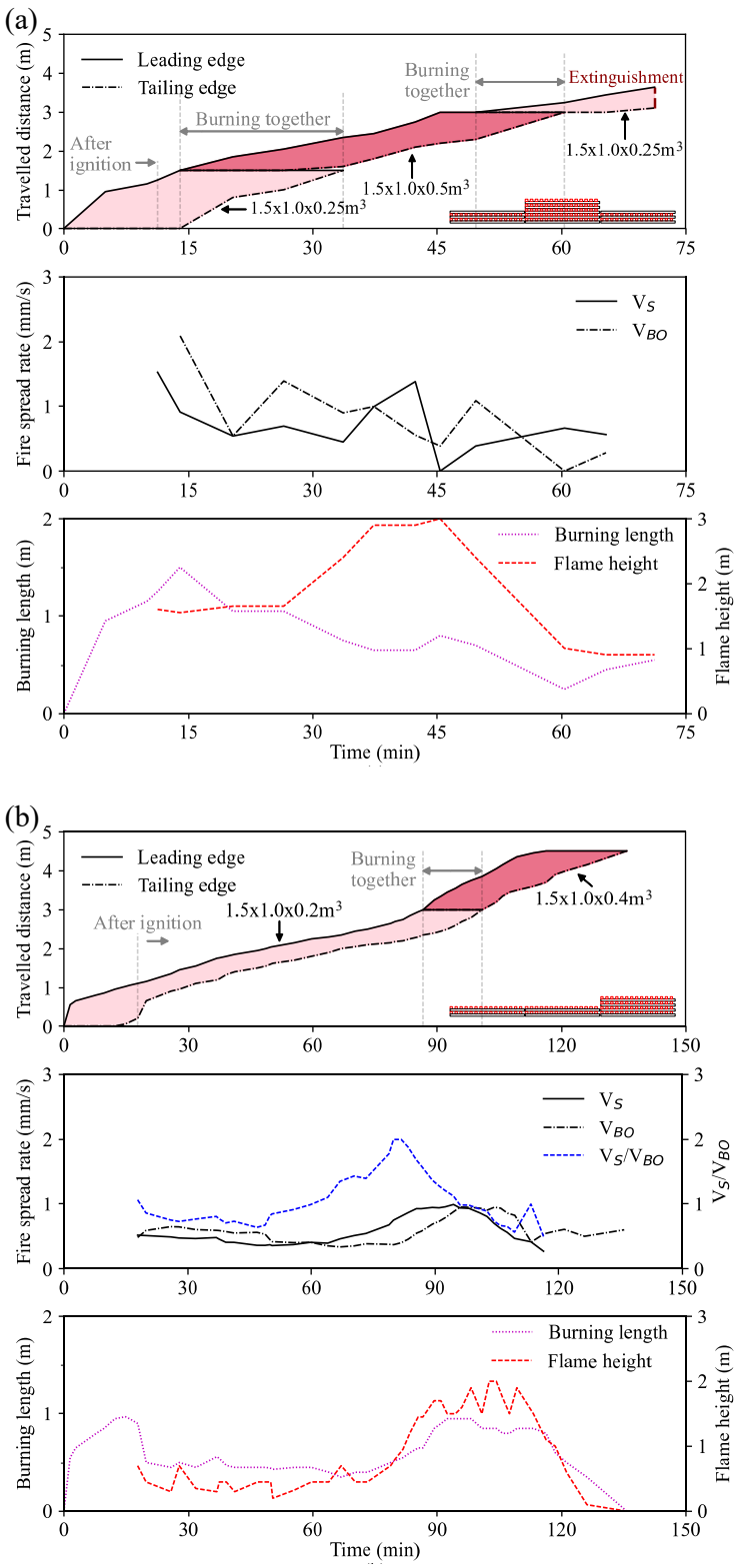

Fig. 9. Summary of burning length, fire spread rate and flame height for fire tests with non-uniform and continuous fuel load distribution. (a) Test 1. (b) Test 2.

In Fig. 10, the characteristic variables of Tests 3-5 can be similarly obtained and illustrated according to the time since ignition. Considering that the fire flames were locally developed in each wood crib stack and spread via fire leaping after ignition, the continuous fire spread rates for tests of the discontinuous wood bed are not observed during the experiments. In Test 3 (Fig. 10(a)), the flame spread rapidly in the Crib 3-1, and then the leading edge propagated to the Crib 3-2 at 9.5 mins and to the Crib 3-3 at 19 mins. The trailing edge appeared only after the wood crib fuel was mostly consumed, i.e., at the decay stage for each crib block. Hence, the trailing edge moved fast in 27-32 mins in the Cribs 3-1 and 3-2.

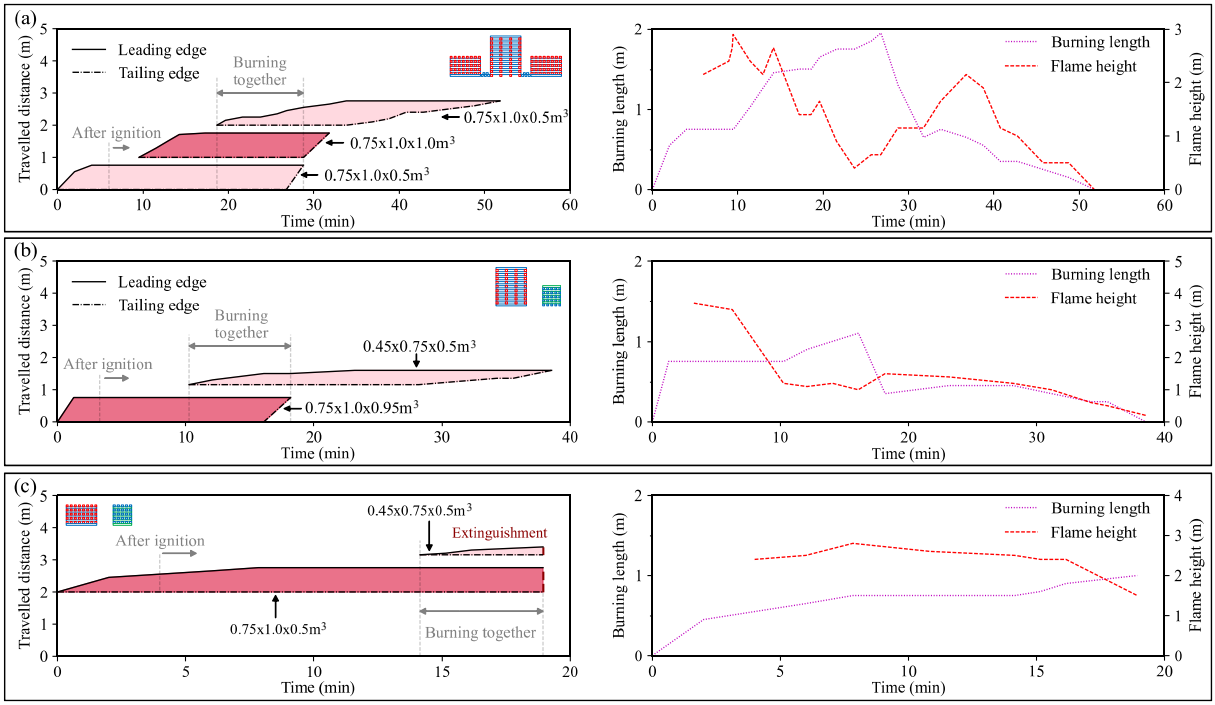

Fig. 10. Summary of burning length, fire spread rate and flame height for fire tests with non-uniform and continuous fuel load distribution. (a) Test 3. (b) Test 4. (c) Test 5.

The observed velocities of leading and trailing edges in Test 3 differ significantly from the fire tests with continuous fuel load (i.e., Test 1 and Test 2). For discontinuous fuel load distribution, due to the gaps between crib blocks, the leading edge leaps from the ignited wood crib to the surrounding wood crib. For instance, after the ignition of Crib 3-1, Crib 3-2 was ignited after around 9 mins under heating from Crib 3-1. After that, within 5 mins the flame spread rapidly over the entire top surface of Crib 3-2. Crib 3-3 was ignited after approx. 18.5 mins under heating from Crib 3-2 and Crib 3-1. But the flame spread relatively slow on Crib 3-3, it took around 15 mins for the leading edge to travel through the top surface of Crib 3-3. Meanwhile, the collapse of a wood crib means decay of the localised fire. In Test 3, when three wood cribs burned together (i.e., 19-29 mins), the burning length was the largest reaching up to 2.0 m, but the flame height was the smallest (less than 0.5 m). It can be explained by three main reasons (1) Crib 3-1 was

collapsed, (2) Crib 3-2 in decaying phase (shorter fire duration due to high porosity), and (3) Crib 3-3 was still in the growing stage. The experimental results of Test 3 demonstrated that the spreading of fire is a complex phenomenon considering the non-uniform fuel load distribution (e.g., gaps between fuels and porosity between wooden sticks).

3.3 Heat release rate

Large compartment fires comprise two components: (1) the fire impact in localised burning region (near field) and non-burning region (far field), (2) the travelling behaviour of localised burning (trajectory and spread rate). In the near field, the fire size of the localised fire is a key index of fire impact, which depends on the fuel load density, the burning length, the heat release rate, Rein et al. [2,31].

During the tests, the MLR of the single wood crib was recorded using the weighing scales. In Fig. 11, the MLR of representative wood crib blocks are presented, which include Crib 2-2 (1.5×1.0×0.2 m^3), Crib3-2 (0.75×1.0×1.0 m^3), Crib 4-2 (0.45×0.75×0.5 m^3) and Crib5-1 (0.75×1.0×0.5 m^3). The measurement uncertainty of mass loss rate is approximately 20%. The Savitzky-Golay filter [32] was used to smooth out fluctuations to present the time-variant MLR during the tests. Meanwhile, the HRR of the corresponding wood crib can be estimated using the MLR data:

$$\dot{Q}'' = \eta \Delta H_c \dot{m}'' \tag{6}$$

where $\dot{Q}''$ is the heat release rate (MW), $\dot{m}''$ is the mass loss rate (kg/s), $\eta \approx 0.8$ is the combustion efficiency following EN 1991-1-2 [28], and ΔH_c = 18 MJ/kg is estimated as the heat of combustion of wood [29].

In Fig. 11(a), the highest HRR (1.58 MW) was found in Crib 3-2, which is of larger spacing of crib (18.5 cm) with a higher stack (1.0 m). On the contrary, the HRR of the Crib 2-2 was much lower (0.2-0.6 MW) and the fire spread on the Crib 2-2 lasted for more than an hour. The effect of porosities of wood cribs has also been investigated by comparing the Crib 3-2 and the Crib 5-1. A numerical study has been conducted by Khan et al. [33] to understand the effect of porosity in a compartment fire. The Crib 3-2 and Crib 5-1 occupied a floor area of 0.75 m × 1.0 m and the same $q_{w,k}$ = 1600 MJ/m^2. However, the porosity of Crib 3-2 (i.e., 0.7223) is higher than Crib 5-1 (i.e., 0.2297). A higher porosity inside the wood crib (Crib 3-2) has enabled a more intense fire (high burning rate) with a shorter duration.

As shown in Fig. 11(a), the peak MLR for the low porosity wood crib 5-1 (0.75×1.0×0.5 m^3 with spacing 5 cm) was approx. 30% lower than the high porosity wood crib 3-2 (0.75×1.0×1.0 m^3 with spacing 18.5 cm), i.e., 0.08kg/s and 0.11kg/s, respectively. For the high porosity wood crib, the MLR decreases drastically after 10 mins, while the fuel was burning steadily for the low porosity wood crib between 4 to 15 mins. Due to high MLR for the high porosity wood crib, the fuel was burnt out much quicker than the low porosity wood crib.

The effect of the porosity of wood cribs on fire-spread behaviours has been further studied in Test 4 (Fig. 10(b)) and Test 5 (Fig. 10(c)). In Test 4, the Crib 4-1 (i.e., 0.75×1.0×0.95 m^3 with spacing 18.5 cm) was ignited. The fire burned locally with a peak flame height of 2.0 m until the fire reached the Crib 4-2 at around 10 mins. Due to the higher porosity (i.e., with spacing 18.5 cm) of the Crib 4-1, the burning duration of the wood crib (0.75×1.0×1.0 m^3) was relatively short. High porosity (i.e., with spacing 18.5 cm) of Crib 4-1 is one of the key reasons for the shorter burning duration of the wood crib (0.75×1.0×1.0 m^3). The porosity (gaps between the sticks) allows air movement between the wooden sticks which may increase the burning rate. As presented in previous studies, the fire may become under-ventilated in the porous region which also may increase the burning rate [13,34]. Furthermore, an expression for the effect of porosity on the burning rate can be found in the SFPE Fire Protection Handbook [35]. The burning rate would be affected by surface area (the higher the surface area exposed to fire, the faster the fuel burns) and height of the fuel, as described in SFPE Handbook [35]. Test 5 shows similar behaviour as Test 4, but in this case, Crib 5-1 (0.75×1.0×0.5 m^3 with spacing 5 cm) had lower porosity (i.e., 2297). The Crib 5-2 was ignited at 15 min, and the Cribs 5-1 and 5-2 burned together until whole fuel was extinguished. The results show that the wood crib with higher porosity can easily ignite the next wood crib, and the fire size would be larger. Meanwhile, comparing the Crib 4-1 and the Crib 5-1, the higher mass flux of the Crib 4-2 was obtained due to the exposure to the large fire size of the Crib 4-1. The higher burning rate not only intensified the radiative flux on the fuel but also accelerated the drying and pyrolysis of wood crib even with a gap of 0.4 m.

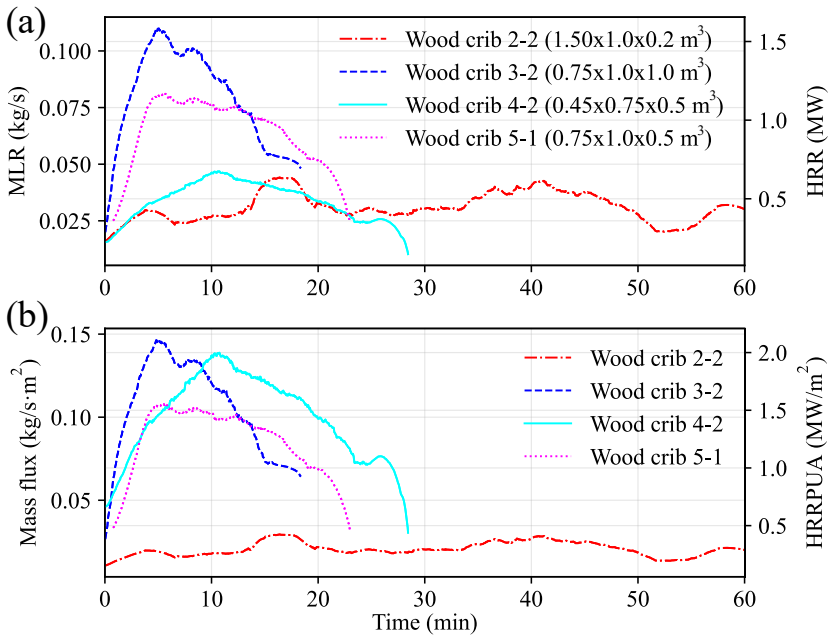

Fig. 11. (a) Recorded MLR and estimated of HRR. (b) Mass flux and heat release rate per unit area (HRRPUA).

In Fig. 11(b), the mass flux is the MLR per unit area on single wood crib (i.e., MLR/A_c) and the HRRPUA is the heat release rate per unit on single wood crib (i.e., HRR/A_c). By considering the mass loss rate per unit floor area, the mass flux of each wood crib can be estimated. It is interesting to see a similar peak mass flux in the Crib 3-2 and the Crib 4-2. The Crib 4-2 has the similar $q_{w,k}$ as of the Crib 3-2 (i.e., 1686 MJ/m^2 and 1600 MJ/m^2 for Crib 4-2 and Crib 3-2 respectively, as shown in Table 3), but lower spacing, which is supposed to burn relatively at slower rate.

With the HRR of the representative wood crib, the total HRR during the fire spread over the wood crib can be calculated. The total HRR indicating the overall fire size is one of the key input parameters for designing travelling fire scenarios [15–17]. For non-uniform and discontinuous fuel load distributions, the total HRR of the spreading fire in large open-plan spaces should account for the combustion of multiple wood cribs. In this section, the time-variant total heat release rates of each fire test are estimated using the mass loss rate calorimetry approach based on the benchmark data of the burning rate of various single wood crib fire tests. Using this approach may result in a high level of uncertainty, for example, as mass loss rates can change due to the radiation of adjacent cribs. Nonetheless, this approach could be used as a rough estimation for illustrative purposes. As shown in Fig. 12, the total HRR variations are presented for tests of continuous fuel and discontinuous fuel separately. The total HRR in Test 1 experienced two peaks (around 1.4 MW), as the middle crib was jointly burning with the Crib 1-1 and the Crib 1-3 at different time steps. In Test 2, the total HRR is averagely lower than in Test 1, and the peak is 1.1 MW after the ignition of the Crib 2-3. The highest total HRR (3.3 MW) occurred in Test 3 after around 23 mins since ignition, which was before the burnt-out of the Crib 3-1 and after the ignition of the Crib 3-3. The total HRR in Test 4 and Test 5 are lower, suggesting that the larger gap significantly delays the ignition of adjacent cribs.

In addition to the HRR histories, the location of fire centre in the representative Tests 2 and 3 are also illustrated in Fig. 12. The fire centre usually indicates the centre of localised heating or the middle between the leading edge and trailing edge, while the slope of location variation represents the fire spread rate. As seen in Fig. 12, the moving of fire centre on a continuous fuel bed in Test 2 is much slower than that in Test 3 with discontinuous wood cribs. The higher fire spread rate is accompanied by the spike of total HRR in Test 2, which suggests the fast-moving of the leading edge. In Test 3, the fire centres correspond to each fire plume on wood crib. The much higher total HRR does come along fast-moving of fire centre, suggesting that the large fire up to 3 MW could stopover for more than 20 min.

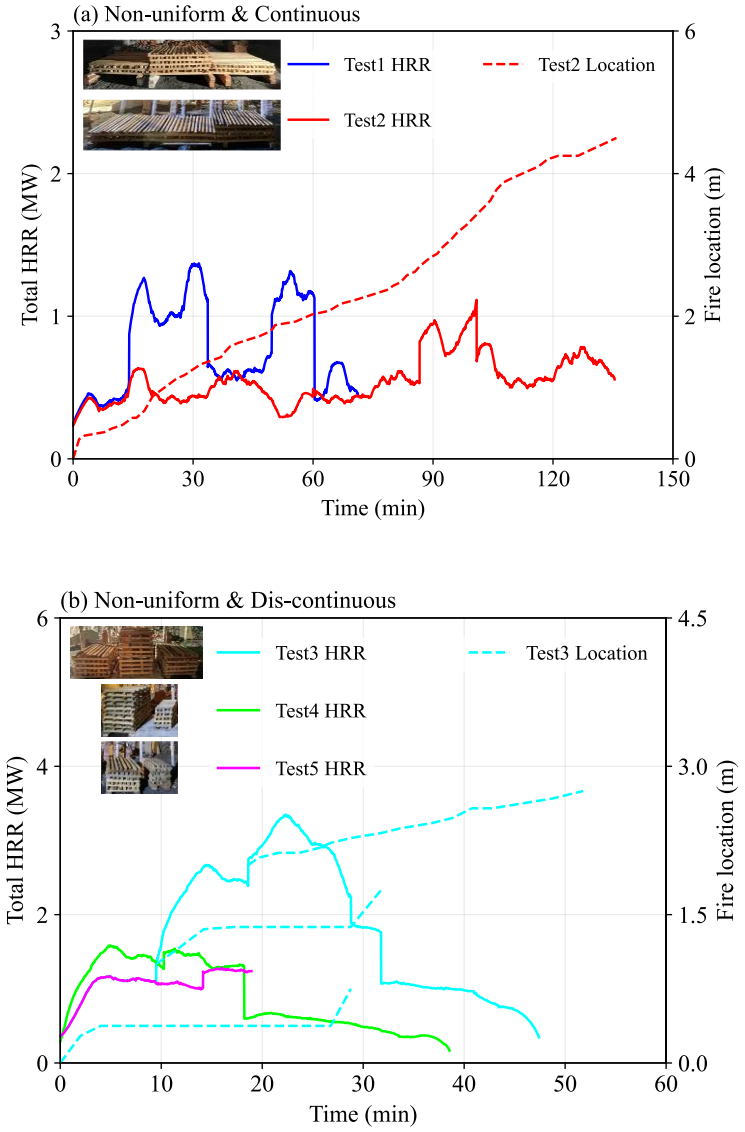

Fig. 12. Estimation of total HRR during the fire tests. (a) Test1 and Test2. (b) Test3, Test4 and Test5.

3.4 Fire impact

The histories of peak gas-phase temperatures at the ceiling level (4.5 m) are an index of the fire impact from the localised burning region. The peak temperatures are extracted from the thermocouples, and the variation curves are plotted in Fig. 13. The data presented in Fig. 13 pertains to the gas temperature, with corrections for radiation errors [36]. For Tests 1 and 2, the peak temperature variation corresponds to the evolution of total HRR. The maximum temperature exceeded 200 °C in Test 1, whereas the highest temperature in Test 2 (lower fuel density) was just above 140 °C. The highest temperature (295 °C) in Test 3 was observed at about 14 mins, where 'multi-centre fire' appeared on Cribs 3-1 and 3-2.

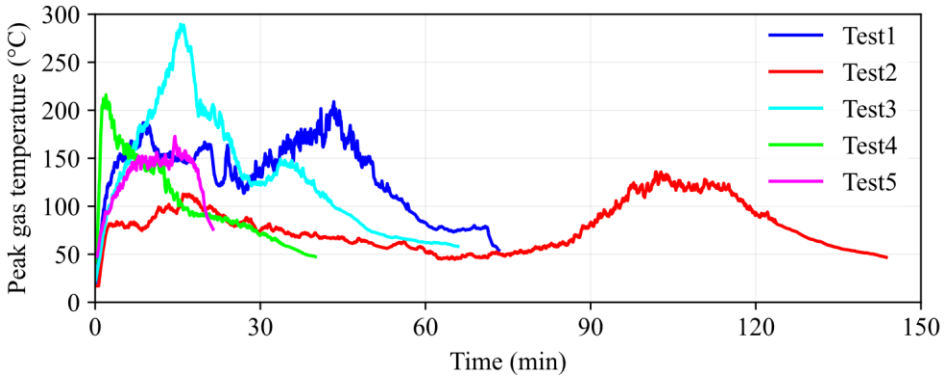

Fig. 13. Peak gas-phase temperature at ceiling in all fire tests.

Fig. 14 further demonstrates the development history of gas-phase temperatures for Test 2 and Test 3. The reason for demonstrating Test 2 and Test 3 in detail is that the two tests have the same fuel load (referring to Table 3), but they represent different typical fuel load distributions. In Test 2, the distribution of wood cribs was non-uniform and continuous, the local fuel load densities were relatively low, i.e., 619 MJ/m^2 or 1238 MJ/m^2 as mentioned in Table 3. In Test 3, the distribution of wood cribs was non-uniform and discontinuous, the local fuel load density was higher, i.e., 1600 MJ/m^2, as mentioned in Table 3. Note, the recorded gas temperatures for all tests were relatively low (see Fig. 13 and Fig. 14), this might be due to the 0.15 m vertical distance between the fuel bed and the thermocouples.

As shown in Fig. 14(a), at 75 mins after ignition in Test 2, the surrounding gas-phase temperature is below 120 °C, meanwhile, the peak ceiling temperature was 50 °C (see Fig. 13). This is due to the modest fire size, i.e., approx. 0.5 MW (see Fig. 12) when the fire spreads to the Crib 2-2 with a low local fuel load density 619 MJ/m^2, which has limited impacts on surroundings. At 90 mins, the peak ceiling temperature increased to 83 °C (see Fig. 13) with an increase of fire size. This is due to the Crib 2-3 was ignited, and the Crib 2-2 and the Crib 2-3 were burning together. At 105 mins, the peak ceiling temperature almost reached the maximum value of around 130 °C, the surrounding gas temperature of the fire was over 180 °C. The rise in the temperatures at 75 mins and 90 mins with the increasing fire sizes was due to the doubled local fuel load density of the Crib 2-3 ($q_{w,k}$ = 1238 MJ/m^2) compared to the Crib 2-2 ($q_{w,k}$ = 619 MJ/m^2). Although there were gaps between the wood cribs in Test 3, the distribution of fuel was more concentrated compared to Test 2, as shown in Fig. 1 and Fig. 2.

The fire duration of Test 3 was significantly shorter than Test 2. It might be due to the higher local fuel load density of Test 3 ($q_{w,k}$ = 1610 MJ/m^2). As shown in Fig. 14(b), at 15 mins, the Crib 3-1 and the Crib 3-2 burn together, the peak ceiling temperature almost reached the maximum value of 290 °C (Fig. 13), and the surrounding gas temperature of the fire was above 200 °C. After 15 mins since ignition, with the gradually burn out of the Crib 3-1 and the Crib 3-2, the gas-phase temperature decreased with the decreasing of fire sizes (Figs. 13 and 14(b)). Although the fire on the Crib 3-3 has been developed at 35

mins, the peak ceiling temperature only re-grown to 145 ºC. This is due to the low porosity of the Crib 3-3 comparing to the Crib 3-2, the fire size of the Crib 3-3 (i.e., approx. at 1.0 MW) was almost half of the Crib 3-2 (i.e., around at 1.5 MW to 2.0 MW) as implied in Fig. 11.

To sum up, the fuel load distribution directly affects the fire development and further affects the spatial temperature field. Therefore, the effect of fuel load distribution should be further studied, e.g., uniform/non-uniform distribution, continuous/discontinuous distribution, global/local density of fuel load, and porosity of fuel.

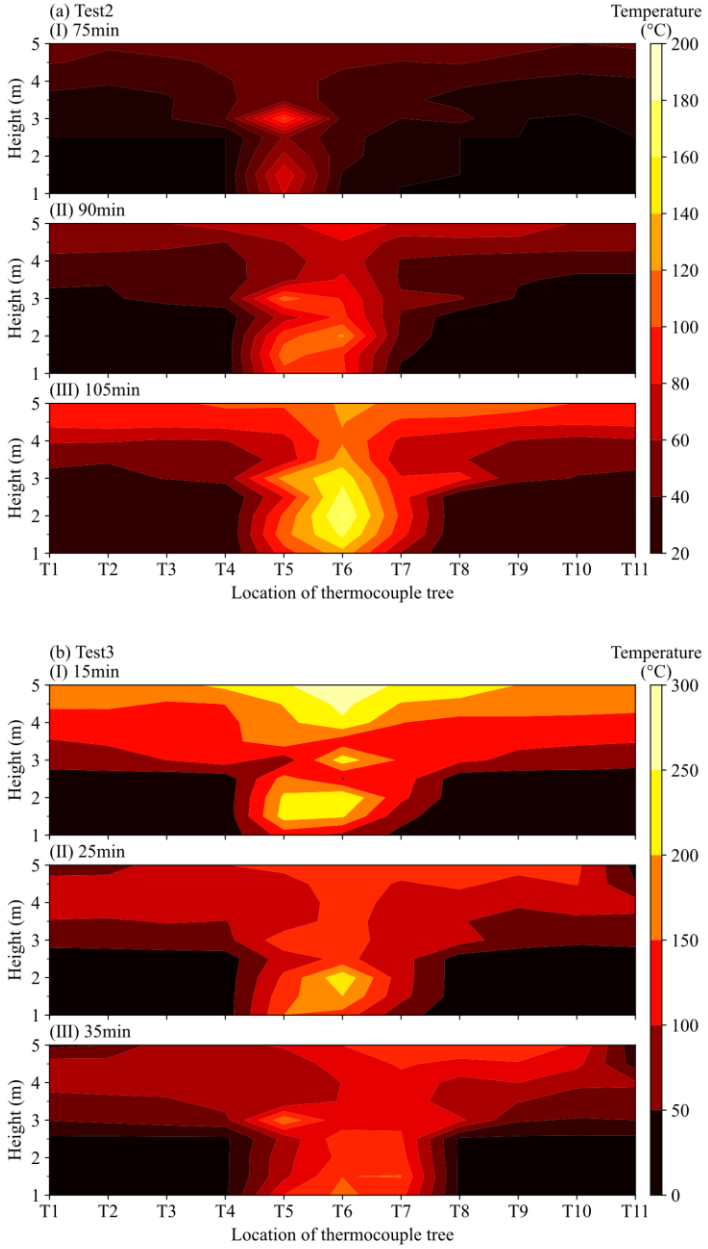

Fig. 14. Gas-phase temperature contour along the line beside the fuel bed with 0.15 m (i.e., the line of the thermocouple trees). (a) Test 2, at 75, 90 and 105 mins. (b) Test 3, at 15, 25 and 35 mins.

Fig. 15 presents the recorded incident heat fluxes measured in Test 2~ 5. The heat fluxes of HF1 and HF2 were given by the heat flux gauges TS-34C and HS-34CB, respectively. Thin skin calorimeters were designed and built as cheaper devices to measure the heat fluxes based on the initial design by Hidalgo et al. [37]. As the fire travels on the fuel bed, the horizontal distance between the heat flux gauges and the flame centre varied. In the meantime, the heat flux measuring devices were subjected to a localised fire of varying size, leading to the changes of heat fluxes as shown in Fig. 15. These data sets provide more fire impact information to a fixed point, indicating the heat fluxes received from an adjacent item and the potential to be ignited spontaneously. It should be noted that fire may not sustain when the fuel bed is discontinuous, such as the gap of 0.4m in Test 4 and Test 5. This suggests in fire safety design, it is feasible to interrupt fire traveling by maintaining clear distance between combustible items and providing sufficient ventilation to avoid smoke accumulation.

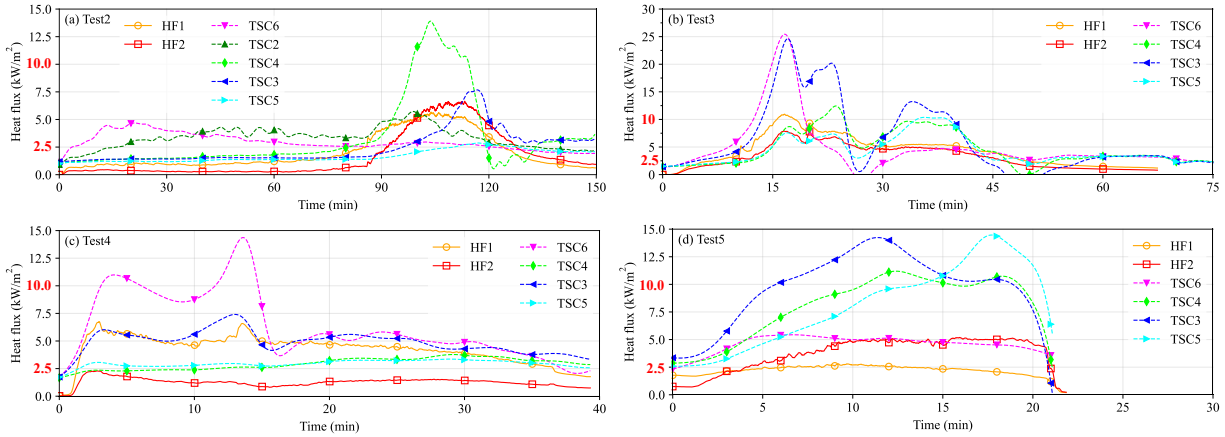

Fig. 15. The recorded incident heat flux of four tests. (a) Test 2. (b) Test 3. (c) Test 4. (d) Test 5.

3.5 Key findings for design fire scenarios

By introducing non-uniform wood crib and discontinuous wood crib in fire testing for travelling fire scenarios, several key findings of the travelling modes are achieved, which can be implemented in establishing more practical design fire scenarios evolving from the current methodologies of assuming uniform fuel bed.

As found in Tests 1 and 2, there are two modes of travelling fire behaviour on non-uniform fuel bed being observed: **Mode I (Travelling):** a ‘travelling fire’ as found in the tests using the uniformly distributed fuel bed [4–9] can be observed. A higher fuel density leads to longer flame band (burning length) during the travelling and the fire spread rate is higher. **Mode II (Re-growing):** The fire grows after a travelling fire behaviour in terms of fire size, when it approaches wood crib of higher fuel density. During this mode, the fire travelling seems to be paused at the wood crib bed, as no move of fire centre occurs but with the increased size and observable higher flame hight.

In Tests 3-5 of discontinuous fuel bed, the following specific modes may be considered in creating worse design fire scenarios. **Mode III (Fire leaping):** The travelling of fire flames is sustained in the form of leaping or jump from the burning wood crib to the adjacent one, which is due to the gap between two wood crib blocks. For fire leaping mode, the travelling can be slower compared to surface spread on continuous fuel bed as the leading wood crib is heated by radiation from the localised fire of a distance. **Mode IV (Multi-centre fire):** After the Mode III of fire leaping, it is likely to have multiple fire plumes located on the wood cribs. In this case, the near field may be approximated by multiple overlapped localised fires, which could cause unknown failure patterns of structural components. Such approximation using multiple localised fire models and the corresponding structural responses certainly need more experimental and numerical investigations.

4. Conclusions

This paper reviews previous travelling fire tests and discusses the limitation and applicability of results of the studies. Previous studies mainly focused on uniform fuel distribution to develop "travelling fire" models. The present study experimentally investigated the effect of non-uniform fuel distribution on fire development in large spaces with sufficient ventilation. The fire-spread behaviour and quantitative characteristics have been presented for five full-scale fire tests. The conclusions are drawn below:

(1) The non-uniform fuel distribution leads fire travelling with various spread rates. The fire-spread behaviour (including fire spread rates and fire sizes) is affected by fuel load density [2,31] and the HRR. With the discontinuous fuel load distribution, the leaping of localised burning between wood cribs may lead to the localised burning with a multi-centre fire.

(2) A series of tests have been conducted for various configurations of wood crib geometries. The experimental results indicate that size of localised burning is affect by the wood crib geometry.

(3) The tests also demonstrate that the porosity affects the HRR. Higher value of HRR is obtained where the gaps were higher between the sticks (i.e., higher porosity of wood crib). The effects of the fuel load density and the porosity of wood cribs should be further studied.

(4) Based on the incident heat fluxes recorded in this study, the critical distance of ignition is evaluated that can be used to present the safe distance from the fire source.

As a conclusion, considering the non-uniform distribution of fuel in performance-based fire safety design, not only can help finding worse design fire scenarios, but also effectively reduce fire risk by adjusting the layout of combustibles.

Acknowledgment

This work is funded by the Hong Kong Research Grants Council Theme-based Research Scheme (T22-505/19-N). The authors also would like to thank the support from Sichuan Fire Research Institute.

Reference

[1] R.G. Gann, A. Hamins, K. Mcgrattan, H.E. Nelson, T.J. Ohlemiller, K.R. Prasad, W.M. Pitts, Reconstruction of the fires and thermal environment in World Trade Center buildings 1, 2, and 7, (2013) 679–707. https://doi.org/10.1007/s10694-012-0288-3.

[2] J. Stern-gottfried, G. Rein, Travelling fires for structural design – Part I : Literature review, Fire Saf. J. 54 (2012) 74–85. https://doi.org/10.1016/j.firesaf.2012.06.003.

[3] X. Dai, S. Welch, A. Usmani, A critical review of "travelling fire" scenarios for performance-based structural engineering, Fire Saf. J. 91 (2017) 568–578. https://doi.org/10.1016/j.firesaf.2017.04.001.

[4] K. Horová, T. Jána, F. Wald, Temperature heterogeneity during travelling fire on experimental building, Adv. Eng. Softw. 62–63 (2013) 119–130. https://doi.org/10.1016/j.advengsoft.2013.05.001.

[5] J.P. Hidalgo, A. Cowlard, C. Abecassis-Empis, C. Maluk, A.H. Majdalani, S. Kahrmann, R. Hilditch, M. Krajcovic, J.L. Torero, An experimental study of full-scale open floor plan enclosure fires, Fire Saf. J. 89 (2017) 22–40. https://doi.org/10.1016/j.firesaf.2017.02.002.

[6] J.P. Hidalgo, T. Goode, V. Gupta, A. Cowlard, C. Abecassis-Empis, J. Maclean, A.I. Bartlett, C. Maluk, J.M. Montalvá, A.F. Osorio, J.L. Torero, The Malveira fire test: Full-scale demonstration of fire modes in open-plan compartments, Fire Saf. J. 108 (2019) 102827. https://doi.org/10.1016/j.firesaf.2019.102827.

[7] J. Sjöström, E. Hallberg, F. Kahl, A. Temple, J. Andersson, S. Welch, X. Dai, V. Gupta, D. Lange, J. Hidalgo, Characterization of TRAvelling FIRes in large compartments, (2019).

[8] E. Rackauskaite, M. Bonner, F. Restuccia, N. Fernandez Anez, E.G. Christensen, N. Roenner, W. Wegrzynski, P. Turkowski, P. Tofilo, M. Heidari, P. Kotsovinos, I. Vermesi, F. Richter, Y. Hu, C. Jeanneret, R. Wadhwani, G. Rein, Fire Experiment Inside a Very Large and Open-Plan Compartment: x-ONE, Fire Technol. (2021). https://doi.org/10.1007/s10694-021-01162-6.

[9] M. Heidari, E. Rackauskaite, E. Christensen, M. Bonner, S. Morat, H. Mitchell, P. Kotsovinos, P. Turkowski, W. Wegrzynski, P. Tofilo, G. Rein, Fire experiments inside a very large and open-plan compartment: x-TWO, in: 11th Int. Conf. Struct. Fire, SiF, Brisbane, 2020. https://doi.org/10.14264/b666dc1.

[10] A.A. Khan, A.S. Usmani, J.L. Torero, Evolution of fire models for estimating structural fire-resistance, Fire Saf. J. (2021). https://doi.org/10.1016/j.firesaf.2021.103367.

[11] A.A. Khan, Z. Nan, L. Jiang, V. Gupta, S. Chen, M.A. Khan, J. Hidalgo, A. Usmani, Model characterisation of localised burning impact from localised fire tests to travelling fire scenarios, J. Build. Eng. 54 (2022) 104601. https://doi.org/10.1016/j.jobe.2022.104601.

[12] Z. Nan, A.A. Khan, L. Jiang, S. Chen, A. Usmani, Application of travelling behaviour models for thermal responses in large compartment fires, Fire Saf. J. 134 (2022) 103702. https://doi.org/10.1016/j.firesaf.2022.103702.

[13] V. Gupta, J.P. Hidalgo, D. Lange, A. Cowlard, C. Abecassis-Empis, J.L. Torero, A review and analysis of the thermal exposure in large compartment fire experiments, Int. J. High-Rise Build. 10 (2021) 345–364.

[14] V. Gupta, A.F. Osorio, J.L. Torero, J.P. Hidalgo, Mechanisms of flame spread and burnout in large enclosure fires, Proc. Combust. Inst. 38 (2021) 4525–4533. https://doi.org/10.1016/j.proci.2020.07.074.

[15] C. Clifton, Fire models for large firecells, HERA Report, 1996.

[16] J. Stern-Gottfried, G. Rein, Travelling fires for structural design-Part II: Design methodology, Fire Saf. J. 54 (2012) 96–112. https://doi.org/10.1016/j.firesaf.2012.06.011.

[17] X. Dai, S. Welch, O. Vassart, K. Cábová, L. Jiang, J. Maclean, G.C. Clifton, A. Usmani, An extended travelling fire method framework for performance-based structural design, Fire Mater. 44 (2020) 437–457. https://doi.org/10.1002/fam.2810.

[18] B.R. Kirby, D. Wainman, L.N. Tomlinson, T. Kay, B.N. Peacock, NATURAL FIRES IN LARGE SCALE COMPARTMENTS, in: Int. J. Eng. Performance-Based Fire Codes, 1999: pp. 43–58.

[19] C. Abecassis Empis, A. Cowlard, S. Welch, J.L. Torero, Chapter 3, Test One: The 'Uncontrolled' Fire, Dalmarnock Fire Tests Exp. Model. (2007) 63–81. http://hdl.handle.net/1842/2411.

[20] X. Huang, Y. Xie, J. Rong, X. Yang, Experimental study of heat release rate of wood crib, Fire Sci. Technol. 33 (2014).

[21] G. Cooke, Tests to determine the behaviour of fully developed natural fires in a large compartment, Fire Note 4, Fire Research Station, Building Research Establishment Ltd, 1998.

[22] D. Rush, X. Dai, D. Lange, Tisova Fire Test – Fire behaviours and lessons learnt, Fire Saf. J. 121 (2021) 103261. https://doi.org/10.1016/j.firesaf.2020.103261.

[23] N. Alam, A. Nadjai, M. Charlier, O. Vassart, S. Welch, J. Sjöström, X. Dai, Large scale travelling fire tests with open ventilation conditions and their effect on the surrounding steel structure – The second fire test, 188 (2022). https://doi.org/10.1016/j.jcsr.2021.107032.

[24] M. Charlier, J. Franssen, F. Dumont, A. Nadjai, O. Vassart, Development of an Analytical Model to Determine the Heat Fluxes to a Structural Element Due to a Travelling Fire, Appl. Sci. (2021).

[25] L.H. Hu, R. Huo, Y.Z. Li, H.B. Wang, Experimental study on the burning characteristics of wood cribs in a confined space, J. Fire Sci. 22 (2004) 473–489. https://doi.org/10.1177/0734904104042595.

[26] D. Gross, Experiments on the Burning of Cross Piles of Wood, J. Reserch Natl. Bur. Stand. Eng. Instrum. 66C (1962) 99–105.

[27] S. McAllister, M. Finney, Effect of Crib Dimensions on Burning Rate, (2013) 533–542. https://doi.org/10.3850/978-981-07-5936-0_08-02.

[28] EN 1991-1-2, Eurocode 1: Actions on structures - Part 1-2: General actions - Actions on structures exposed to fire, Eur. Commitee Stand. (2005).

[29] CIBSE Guide E, Fire Safety Engineering, Fourth, The Chartered Institution of Building Services Engineers, London, 2019.

[30] J.G. Quintiere, Principles of fire behavior, Second, Taylor & Francis, CRC Press, Boca Raton, FL, 2016. https://doi.org/10.1201/9781315369655.

[31] E. Rackauskaite, C. Hamel, A. Law, G. Rein, Improved Formulation of Travelling Fires and Application to Concrete and Steel Structures, Structures. 3 (2015) 250–260. https://doi.org/10.1016/j.istruc.2015.06.001.

[32] J.E.J. Staggs, Savitzky-Golay smoothing and numerical differentiation of cone calorimeter mass data, Fire Saf. J. 40 (2005) 493–505. https://doi.org/10.1016/j.firesaf.2005.05.002.

[33] M.A. Khan, A.A. Khan, A.S. Usmani, X. Huang, Can fire cause the collapse of Plasco Building: A numerical investigation, Fire Mater. (2021) 1–16. https://doi.org/10.1002/fam.3003.

[34] C. Heskestad, Modeling of enclosure fires, Symp. Combust. 14 (1973) 1021–1030. https://doi.org/10.1016/S0082-0784(73)80092-X.

[35] M.J. Hurley, D.T. Gottuk, J.R. Hall Jr., K. Harada, E.D. Kuligowski, M. Puchovsky, J.L. Torero, J.M. Watts Jr., C.J. WIECZOREK, SFPE Handbook of Fire Protection Engineering, NY: Springer New York, New York, 2016.

[36] L.G. Blevins, W.M. Pitts, Modeling of bare and aspirated thermocouples in compartment fires, Fire Saf. J. 33 (1999) 239–259. https://doi.org/10.1016/S0379-7112(99)00034-X.

[37] J.P. Hidalgo, C. Maluk, A. Cowlard, C. Abecassis-Empis, M. Krajcovic, J.L. Torero, A Thin Skin Calorimeter (TSC) for quantifying irradiation during large-scale fire testing, Int. J. Therm. Sci. 112 (2017) 383–394. https://doi.org/10.1016/j.ijthermalsci.2016.10.013.

Appendix

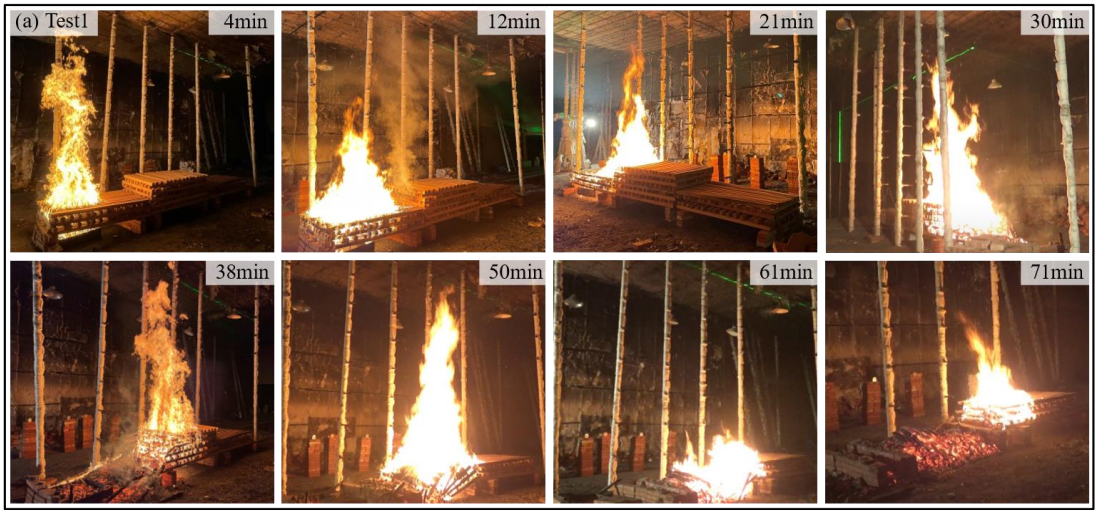

Fig. A1. Fire spread on continuous fuel bed (Test 1).

Fig. A2. Fire spread on continuous fuel bed (Test 2).

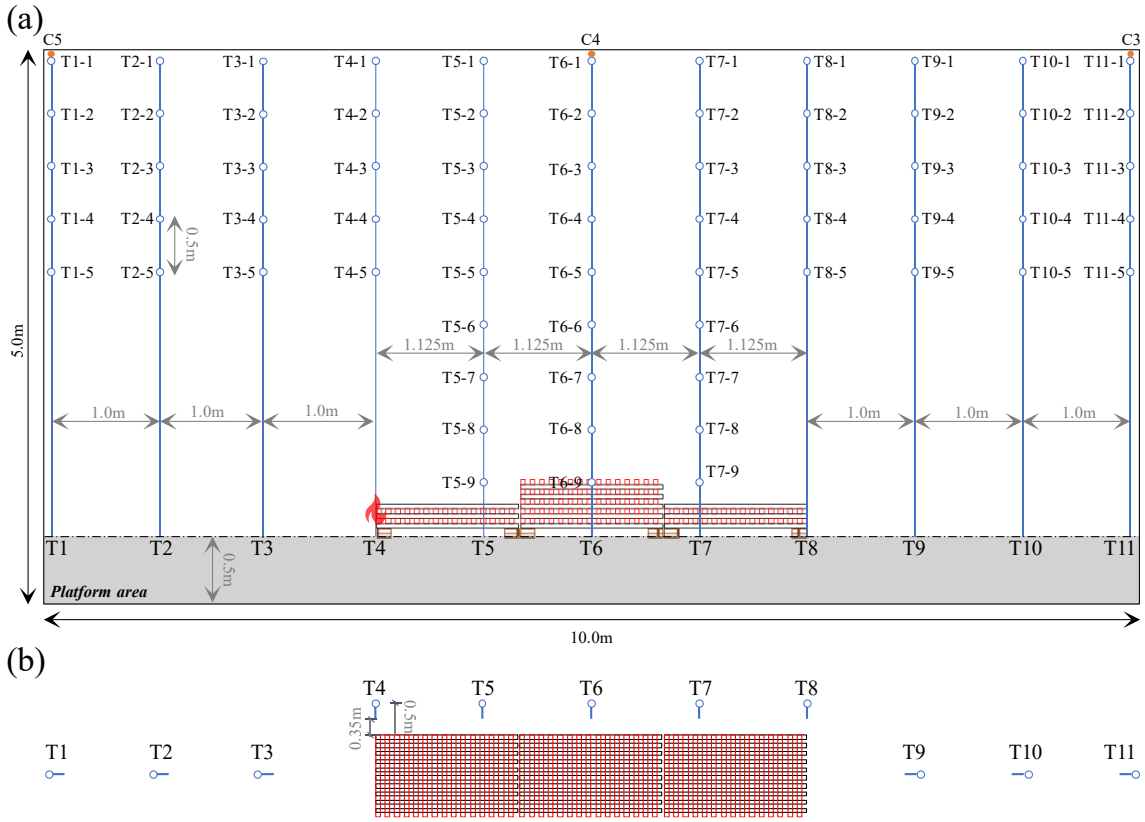

Fig. A3. The sketch of the experimental set-up of Test 1 with the location of sensors. (a) Elevation view. (b) Plan view.

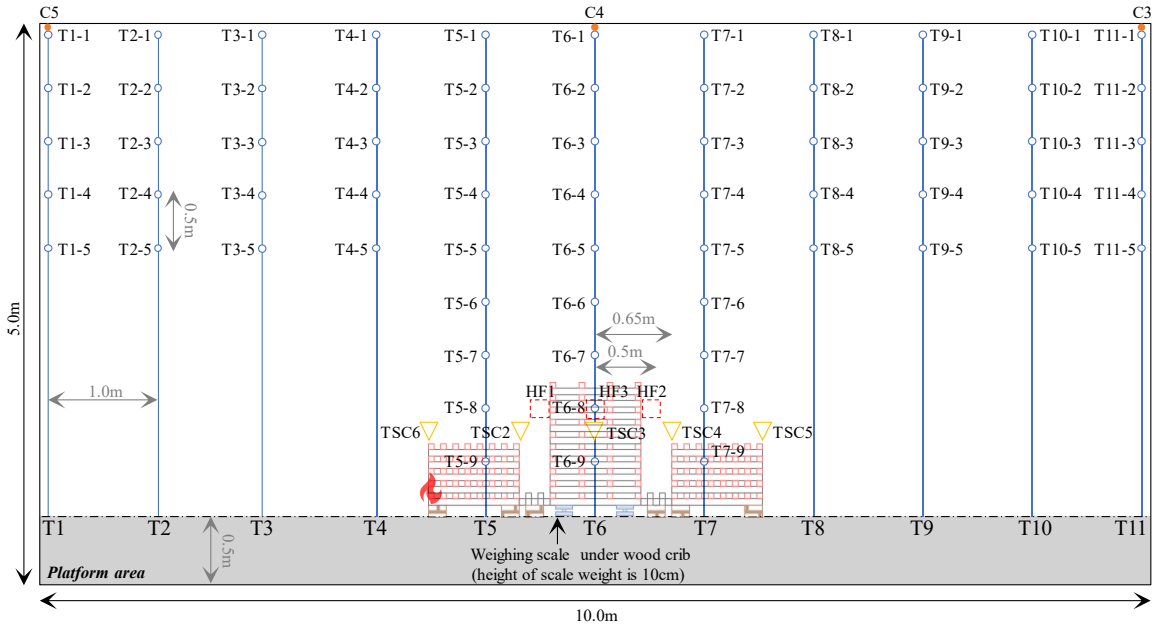

Fig. A4. The sketch of the experimental set-up of Test 3 with the location of sensors.

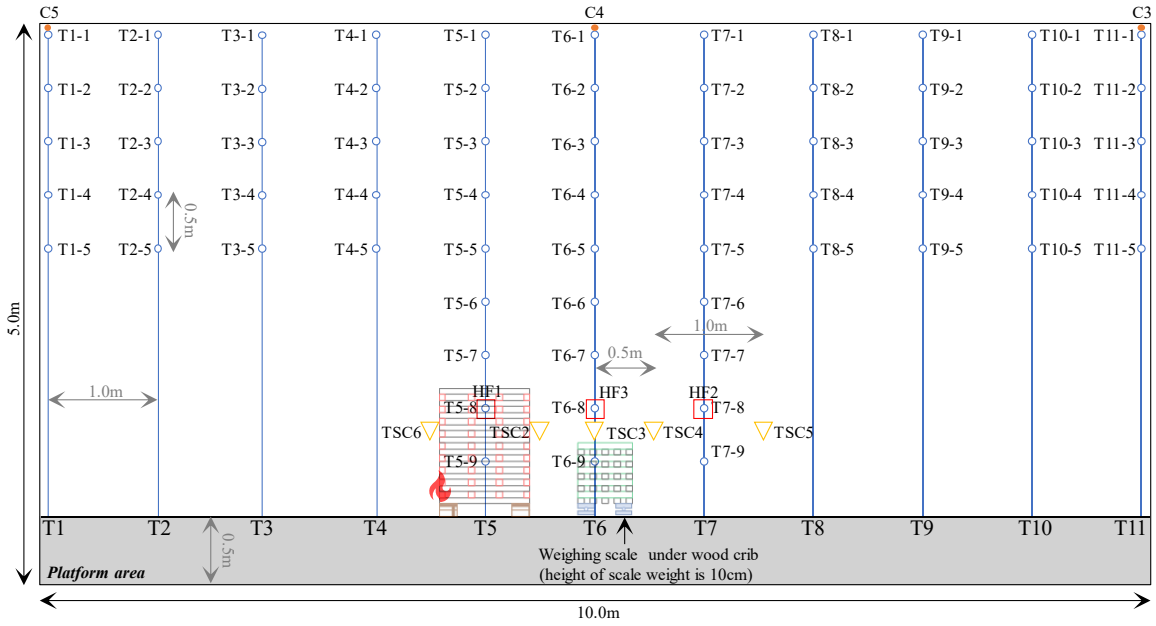

Fig. A5. The sketch of the experimental set-up of Test 4 with the location of sensors.

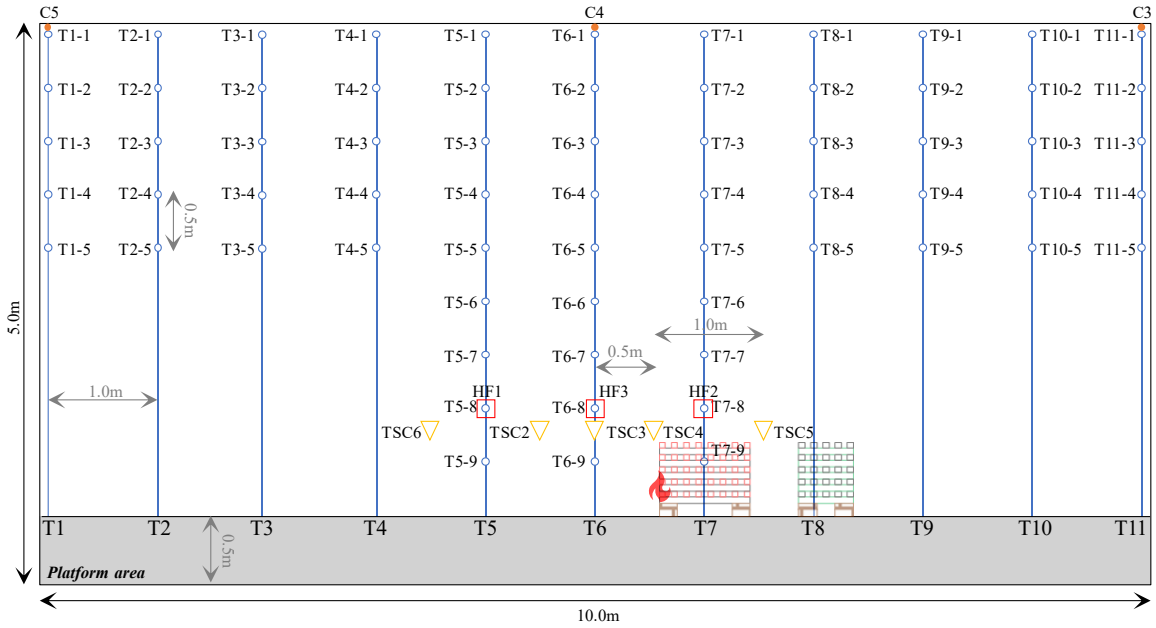

Fig. A6. The sketch of the experimental set-up of Test 3 with the location of sensors.

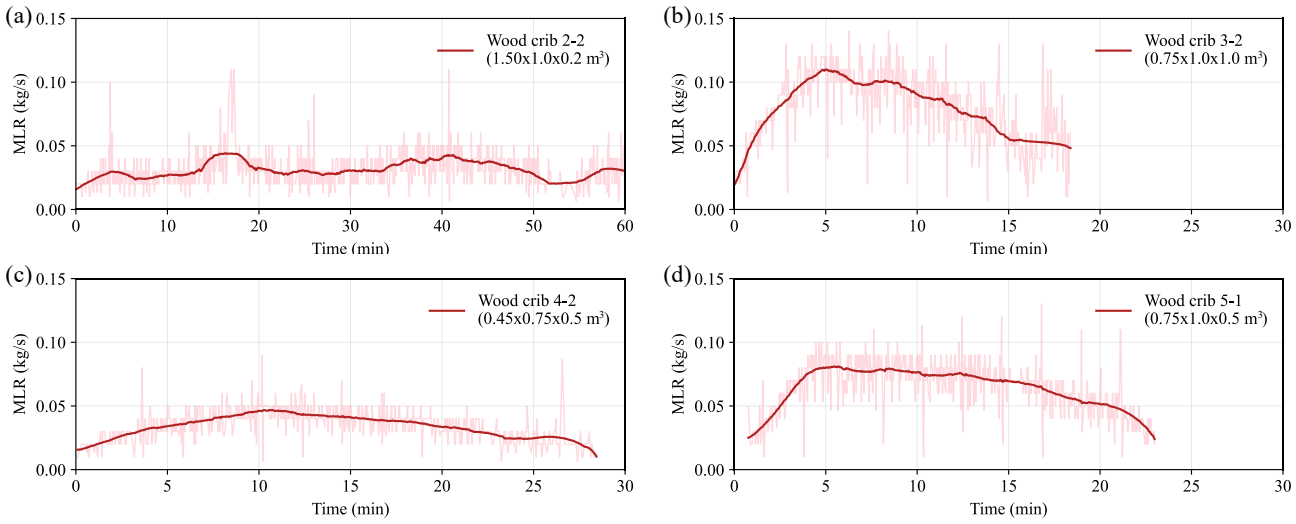

Fig. A7. The measurement of mass loss rate of the wood cribs. (a) Wood crib 2-2. (b) Wood crib 3-2. (c) Wood crib 4-2. (d) Wood crib 5-1.